

3.9GHz SCRF Deflecting Cavity Input Coaxial Cable Choice A Combined Thermal and Electromagnetic Heat Load Calculation

T.Berenc, R.Rabehl, Allan Rowe
6/8/2005

Abstract: *A heat load analysis which incorporates electrical conductivity dependence upon temperature is presented. The analysis was used to choose an input coupler coaxial cable for the superconducting RF (SCRF) 3.9GHz Deflecting Cavity. The work presented here was performed approximately 3 years ago now, but there has been a renewed interest to document the results and information gained during this work.*

Introduction

The 3.9GHz superconducting RF (SCRF) Deflecting Cavity is driven by a highly over-coupled input coupler in order to control the cavity energy in the presence of microphonics and Lorentz force detuning effects. Due to the high input coupling coefficient the RF dissipated power associated with the forward and reflected waves on the input transmission line are of the same order of magnitude as the RF energy dissipated within the cavity walls. Thus, the heat load which the transmission line geometry presents to the cryogenic system becomes important to the cryostat design. Fortunately, this heat load is intercepted at a higher temperature than the cavity; at an 80K intercept as opposed to the $\sim 1.8\text{K}$ cavity temperature.

The heat load analysis presented here combines the RF loss equations and the thermal load calculations to take into account the electrical conductivity dependence upon temperature for the simple geometry of a coaxial input transmission line. The results of this analysis are used to choose a commercially available coaxial cable and its physical arrangement within the cryostat.

The Geometry

The RF input coupler is a coaxial geometry, consisting of a vacuum-dielectric portion near the cavity followed by a commercially available coaxial cable which provides RF drive from outside the cryostat. A sketch of the proposed arrangement is shown in Fig.1. The arrangement resides within the vacuum space of the cryostat. The outside of the cryostat is at room temperature while the cavity-side of the coaxial cable is tied to an 80K intercept.

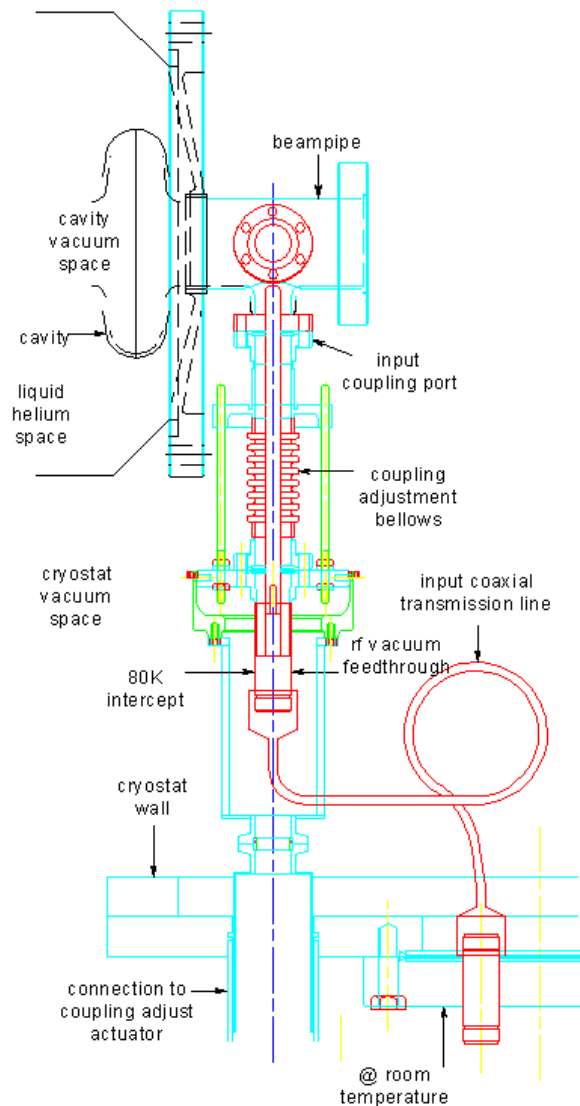


Figure 1: Input Coupler Geometry

The final design routes the cable and room temperature feedthrough coincident with the axis of the input coupler; thus allowing for a straight cable.

The RF and thermal considerations dictate conflicting requirements to minimize the heat load. A long cable is ideal for minimizing thermal conduction losses between the room temperature cryostat wall and the 80K intercept while a short coaxial cable is ideal for minimizing RF losses. Similarly, the cable diameter choice and the selection of cable materials present conflicting RF and thermal considerations. Thus, a design that minimizes the heat load should exist for some intermediate cable length and cable size with suitable cable materials.

Commercially Available Coaxial Cable

Five sources of coaxial cable were reviewed; Andrew Corporation, Micro-Coax, Times Microwave Systems, Precision Tube, and Meggitt Safety Systems (see Ref. [6]-[10]). From these there are many types of coaxial cable which differ in construction and materials.

Construction & Conductor Materials

There are a few different construction styles offered. The semi-rigid type can be bent and shaped, but is not designed for flexibility. There is a hand-formable semi-rigid type cable whose solid outer conductor is made from either aluminum or a high purity copper. This cable type offers flexibility while not sacrificing high-frequency shielding. There also is a braid-over-foil wrap flexible cable type. Finally, a corrugated solid outer conductor flexible cable is available [9].

The outer and inner conductors can be made either of a single material or of a clad and/or coated type construction consisting of multiple materials. These plated materials allow for good RF surface resistance with a low total thermal conductivity.

Dielectric Materials & Radiation Effects

Most of the commercially available cable is made from a Teflon* based dielectric; either a high-density solid form of polytetrafluoroethylene (PTFE) or a low-density PTFE. Polyethylene dielectrics can also be found from Andrew and Times Microwave. In terms of resistance to radiation, polyethylene is much better than Teflon. Teflon is an extremely poor radiation resistant material.

Some alternative dielectric materials that are available for coaxial cable are Tefzel, Kapton, magnesium

oxide (MgO), and silicon dioxide (SiO₂). Tefzel has good resistance to radiation, but has high RF losses. Furthermore, its relative dielectric constant is much greater than 1.0; usually >2.1. Therefore, the cable requires non-standard connector geometries which are very difficult to find; thus requiring custom designs. Kapton's dielectric constant is also high.

Tefzel is being used in the construction of cables sold as "spaceflight" cables. However, the Tefzel is used only on the jacket material while Teflon is still used in the dielectric. It is not clear how well this Tefzel can truly shield the dielectric from neutrons. Since the dielectric is still Teflon, this cable was not considered. Some companies do offer Tefzel as the dielectric, but it was not considered because of its high RF losses.

Studies found in literature have found that inorganic materials are generally more resistant to radiation than organic materials; thus MgO and SiO₂ are good choices for a dielectric in a radiation resistant cable. See references [11] and [12].

It was difficult to find MgO dielectric cable. However, many manufacturers are now offering SiO₂ cable for phase stable applications in aircraft and space designs; including Times Microwave as well as Meggitt Safety Systems.

Both of these materials have relative dielectric constants close to unity; thus standard connectors can be used. However, they both are hygroscopic (readily absorb moisture). According to Ref. [11], "many materials are more resistant to radiation in the absence of oxygen or moisture and at lower temperatures." The remedy to this hygroscopic property is to use hermetic connectors during the cable fabrication process and not to let raw cable sit around in storage without being sealed. The downside to this is that the connectors dominate the cost of the cable assemblies.

The Analysis Model

A block diagram of the analysis model used for both the inner and outer conductors of the input coaxial transmission line is shown in Fig.2. Each conductor of the cable is segmented into n segments each with an average temperature, T_n ; the first and last segments being $\frac{1}{2}$ the length of the other segments. The temperature boundary conditions are the room

* Trade name of E.I. DuPont de Nemours & Company.

temperature plane and the 80K intercept plane. The heat generated within each segment, q_{gen} , is due to the power dissipated in that conductor-segment as a result of providing power, P_L , to the RF load at the 80K-intercept end of the cable while overcoming the temperature dependent energy losses of the cable. Thus, the solution of the total RF cable losses and the total heat flow rate into the 80K intercept involves the solution of the heat flow equations and the RF loss equations which are coupled through the equilibrium temperature profile of the cable. The solution of this general type of problem is simplified in this case by the coaxial geometry.

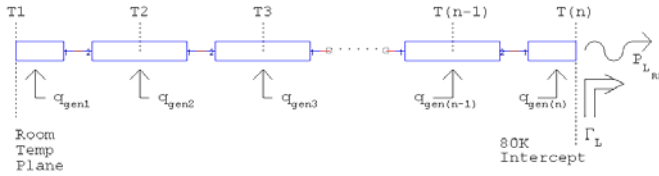


Figure 2: Analysis Model Block Diagram

The RF losses take into account the attenuation of both the forward and reflected waves on the transmission line. The attenuation due to conductive losses on both the inner and outer conductors is calculated by a classical perturbation technique while using temperature-dependent resistivity data from [1] and [2]. The attenuation due to dielectric losses is calculated from the Taylor series expansion of the complex propagation constant using the loss tangent value of the dielectric material. Both techniques are explained in [3].

The temperature-dependent resistivity data from [1] and [2] showed that over the 80K-300K temperature range, the resistivity of the metals used for the cable conductors could be approximated by a simple linear function of temperature. Thus, a least-squares regression line was used to model the resistivity over this temperature range.

No temperature-dependent data was found for the dielectric loss-tangent of solid Teflon, thus the room-temperature value from [3] was used. The low-density Teflon dielectric loss-tangent was calculated by multiplying the loss-tangent data of solid Teflon by

the ratio of the dissipation factors of solid Teflon and low-density Teflon as stated in [6].

The continuous RF power levels were based upon the power needed in the 13-cell cavity of shape C15 for a 5MV/m deflecting gradient assuming a Q_o of 2.1×10^9 and a Q_{ext} of 6×10^7 . A review of the required power levels for these conditions can be found in [4]. An additional 0.4W of RF power was added to the cavity power to account for the power dissipation in the air-dielectric bellows section between the coaxial cable and the cavity. This 0.4W was calculated based upon a separate thermal and electromagnetic analysis of the bellows section. Thus, the total continuous RF power that needs to be supplied to the load at the cavity-end of the coaxial cable is theoretically 4.65W using the above design values. The reflection coefficient magnitude at the input to the bellows section is roughly 0.94.

The heat transfer analysis is based on application of an energy balance to the inner and outer conductors at each node. The energy balance consists of terms representing heat conduction into the node, heat conduction out of the node, and heat generation due to RF losses.

The heat conduction terms use temperature-dependent thermal conductivities calculated by user-written libraries within the EES software package. Data and equations for these property libraries are collected from various sources. Among the sources used are publications such as the *Thermophysical Properties of Matter* series and the National Institute of Standards [13].

The dielectric is treated differently than the conductors. Longitudinal heat conduction resistance along the Teflon dielectric is about twice that of radial heat conduction resistance so only radial heat transfer in the dielectric is considered. Making the simplification that the RF losses within the dielectric are volumetrically uniform throughout its cross-section, the radial temperature profile of the dielectric can be analytically determined using the temperatures of the inner and outer conductors as boundary conditions. Heat transfer rates between the dielectric and the conductors are then calculated from the temperature profile.

The equation set combining the RF and thermal equations can be found in a sample EES equation set in Appendix A. A 100-node coaxial cable model results in a set of 3811 equations, approximately 3500 of which must be solved simultaneously. A sample result of a simulation is shown in Figure 3.

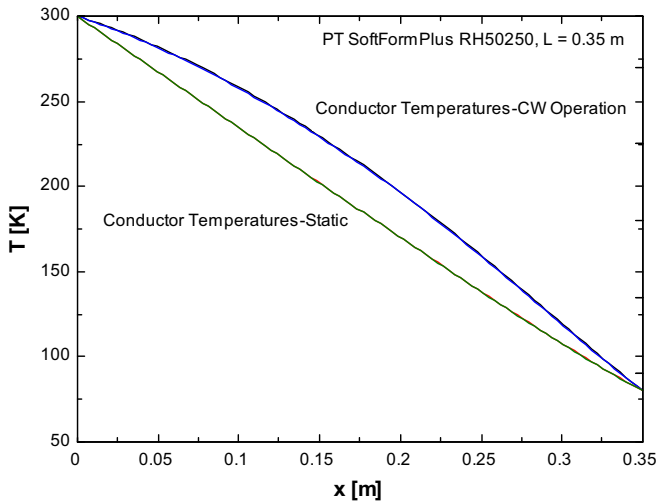


Figure 3: A sample result from a thermal analysis.

Before making the final choice for the cable, many Teflon dielectric cables were simulated. Appendix B summarizes those simulations.

Cable Choice

SiO₂ cable was chosen. The design requirement was that no poor radiation resistant material be used, especially Teflon, since the cavity will be installed in a radiation environment. Although detailed information about radiation doses and project lifetime were not readily available, the cost of downtime caused by even a single failure due to radiation damage could far exceed the cost of the cable.

The SiO₂ cables offered from [10] were simulated. The specific cable which had a low heat load for a practical installation length of 0.27 meters was the 0.275” diameter cable. Figure 4 shows the simulated heat load as a function of cable length for three conditions: a static (no RF) condition, a 1/3 duty factor condition, and a continuous wave (CW) RF condition.

This cable was also reviewed for multipacting issues at our power levels using Ref. [14]. It should be

multipacting free in a standing wave condition for incident power levels into the tens of kW range. Ideally this cable should only have to support approximately 40W of incident power.

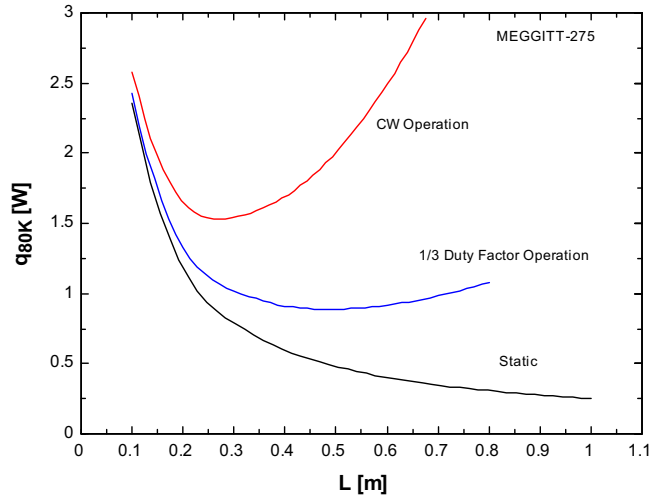


Figure 4: Heat Load to the 80K shield as a function of cable length for the 0.275” SiO₂ cable.

At the time of the order for this cable, Meggitt had 0.270” cable stock; thus the cable which was ordered was 0.270”. The details of the cable assembly can be found in Fermilab drawing number 1620.200-MD-398361. The cable itself is constructed from a Copper over Niobium over 316 Stainless Steel center conductor, a 304 Stainless Steel over Copper jacket outer conductor, with 316 Stainless Steel Type N connectors.

Simulations of the other SiO₂ cable diameter sizes can be found in Appendix C.

Summary

An analysis of the heat load presented by the RF input coaxial cable configuration for the 3.9GHz Deflecting Cavity was performed using a model that took into account temperature-dependent electrical and thermal conductivities. SiO₂ cable was chosen for the deflecting cavity input coupler cabling. A review of commercially available coaxial cables was documented to aid in the selection for other projects. Material that can be found in the references listed includes information pertaining to coaxial cables, radiation effects on materials, and material properties.

References

- [1] Battelle Memorial Institute, Metals and Ceramics Information Center, *Handbook on materials for superconducting machinery; mechanical, thermal, electrical, and magnetic properties of structural materials*, Sponsored by Advanced Research Projects Agency; Contract monitor: Cryogenics Division, National Bureau of Standards, Boulder, Colorado. Columbus, Ohio, 1974.
- [2] United States, National Bureau of Standards. Cryogenic Engineering Laboratory, Boulder, Colo., *A compendium of the properties of materials at low temperature (Phase II)* General editors: R.B. Stewart & V.J. Johnson., Wright-Patterson Air Force Base, Ohio, United States Air Force, Air Force Systems Command, Aeronautical Systems Division, 1961.
- [3] D.M.Pozar, *Microwave Engineering*, 2nd Edition, John Wiley & Sons, N.Y. 1998.
- [4] T.Berenc, “Kaon Separator RF Drive Power Requirements”, Fermilab RFI Note #025, 14Jan.2002, <<http://www-rfi.fnal.gov/technotes/TN/TN025.pdf>>.
- [5] Precision Tube, Coaxitube Division, “Semi-Rigid & Flexible Coaxial Cables & Assemblies”, 2001, <<http://www.precisiontube.com>>.
- [6] Micro-Coax, “Semi-Rigid Coaxial Cable”, Aug. 2000, <<http://www.micro-coax.com>>.
- [7] Micro-Coax, “UtiFlex: Flexible Microwave Cable Assemblies”, SSDW20M, Dec. 1998.
- [8] Times Microwave Systems, “Complete Coaxial Cable Catalog & Handbook”, Catalog TL-14, April 2001, <<http://www.timesmicrowave.com>>.
- [9] Andrew Corporation, “Catalog 38”, pp.440-635, 2000, <<http://www.andrew.com>>.
- [10] Meggitt Safety Systems Inc. <<http://www.stablecable.com>>.
- [11] M.Awschalom and T.Borak, “The Effect of Radiation on Electrical Insulating Materials”, Fermilab Technical Memo TM-183, 08Aug1969. *Note: This is really a copy of an abstract from the Radiation Effects Information Center: C.L. Hanks, D.J. Hamman, REIC Report No. 46, Battelle Memorial Institute, Columbus, OH.*
- [12] CERN Report 89-12.
- [13] National Institute of Standards and Technology (NIST) Cryogenic Technologies Group Material Properties web page
http://cryogenics.nist.gov/NewFiles/material_properties.html
- [14] E.Somersale, P. Yla-Oijala, & D.Proch, “Analysis of Multipacting in Coaxial Lines”, Proceeding of the 1995 Particle Accelerator Conference , Vol.3 pp.1500-1502.

APPENDIX A

CKM COAXIAL CABLE MODEL

INPUTS

Cable

n = 100 number of nodes

L = 0.35 m; length of cable

Outer Conductor-Geometry

$$OR_{oc} = \frac{6.35}{2} \cdot \left[0.001 \cdot \frac{m}{mm} \right] \quad \text{m; outer radius of outer conductor}$$

$$IR_{oc} = \frac{5.461}{2} \cdot \left[0.001 \cdot \frac{m}{mm} \right] \quad \text{m; inner radius of outer conductor}$$

$$t_{oc,plating} = 0.003 \cdot \left[0.0254 \cdot \frac{m}{in} \right] \quad \text{m; thickness of plating}$$

Outer Conductor-Materials and Thermal Properties

$oc_{plated} = 0$ plating flag: 0 = not present, 1 = present

$k_{oc,core,i} = \mathbf{al1100k}(T_{oc,i})$ for $i = 1$ to n W/m-K; thermal conductivity of outer conductor core material

$k_{oc,plating,i} = \mathbf{ss304k}(T_{oc,i})$ for $i = 1$ to n W/m-K; thermal conductivity of outer conductor plating material

Outer Conductor-RF Properties

$\rho_{oc,i} = \mathbf{al1100RRR14elecresistivity}(T_{oc,i})$ for $i = 1$ to n

Inner Conductor-Geometry

$$OR_{ic} = \frac{2.0447}{2} \cdot \left[0.001 \cdot \frac{m}{mm} \right] \quad \text{m; outer radius of inner conductor}$$

$$t_{ic,cladding} = 0.0015 \cdot \left[0.0254 \cdot \frac{m}{in} \right] \quad \text{m; thickness of cladding}$$

$$t_{ic,plating} = 0.003 \cdot \left[0.0254 \cdot \frac{m}{in} \right] \quad \text{m; thickness of plating}$$

Inner Conductor-Materials and Thermal Properties

$ic_{clad} = 0$ cladding flag: 0 = not present, 1 = present

$ic_{plated} = 1$ plating flag: 0 = not present, 1 = present

$k_{ic,core,i} = \mathbf{CuOFHck}(T_{ic,i})$ for $i = 1$ to n W/m-K; thermal conductivity of inner conductor core material

$k_{ic,cladding,i} = \mathbf{CuOFHck}(T_{ic,i})$ for $i = 1$ to n W/m-K; thermal conductivity of inner conductor cladding material

$k_{ic,plating,i} = \mathbf{agk}(T_{ic,i})$ for $i = 1$ to n W/m-K; thermal conductivity of inner conductor plating material

APPENDIX A

Inner Conductor-RF Properties

$$\rho_{c,i} = \text{agelecreisistivity}(T_{ic,i}) \quad \text{for } i = 1 \text{ to } n$$

Dielectric-Geometry

$$IR_D = OR_{ic} \quad m; \text{ inner radius of dielectric}$$

$$OR_D = IR_{oc} \quad m; \text{ outer radius of dielectric}$$

Dielectric-Thermal Properties

$$k_{D,i} = \text{teflonk} \left[\frac{T_{ic,i} + T_{oc,i}}{2} \right] \quad \text{for } i = 1 \text{ to } n \quad W/m-K; \text{ thermal conductivity of dielectric material}$$

Dielectric-RF Properties

$$\alpha_D = 0.0068$$

THERMAL MODEL

Cable

$$dL = \frac{L}{n-1} \quad m; \text{ nodal length}$$

$$x_1 = 0$$

$$x_i = x_{i-1} + dL \quad \text{for } i = 2 \text{ to } n$$

Outer Conductor-Geometry

$$A_{oc,plating} = \pi \cdot (OR_{oc}^2 - (OR_{oc} - oc_{plated} \cdot t_{oc,plating})^2) \quad m^2; \text{ cross-sectional area of plating}$$

$$A_{oc,core} = \pi \cdot ((OR_{oc} - oc_{plated} \cdot t_{oc,plating})^2 - IR_{oc}^2) \quad m^2; \text{ cross-sectional area of core}$$

Outer Conductor-Energy Balances

$$T_{oc,1} = 300 \quad K; \text{ room-temperature end of cable}$$

$$q_{in,oc,plating,i} + q_{in,oc,core,i} + q_{gen,oc,i} + q_{D,oc,i} = q_{out,oc,plating,i} + q_{out,oc,core,i} \quad \text{for } i = 2 \text{ to } n-1$$

$$q_{in,oc,plating,i} = oc_{plated} \cdot \left[\frac{k_{oc,plating,i-1} + k_{oc,plating,i}}{2} \right] \cdot A_{oc,plating} \cdot \left[\frac{T_{oc,i-1} - T_{oc,i}}{dL} \right] \quad \text{for } i = 2 \text{ to } n-1$$

$$q_{in,oc,core,i} = \left[\frac{k_{oc,core,i-1} + k_{oc,core,i}}{2} \right] \cdot A_{oc,core} \cdot \left[\frac{T_{oc,i-1} - T_{oc,i}}{dL} \right] \quad \text{for } i = 2 \text{ to } n-1$$

$$q_{out,oc,plating,i} = oc_{plated} \cdot \left[\frac{k_{oc,plating,i} + k_{oc,plating,i+1}}{2} \right] \cdot A_{oc,plating} \cdot \left[\frac{T_{oc,i} - T_{oc,i+1}}{dL} \right] \quad \text{for } i = 2 \text{ to } n-1$$

$$q_{out,oc,core,i} = \left[\frac{k_{oc,core,i} + k_{oc,core,i+1}}{2} \right] \cdot A_{oc,core} \cdot \left[\frac{T_{oc,i} - T_{oc,i+1}}{dL} \right] \quad \text{for } i = 2 \text{ to } n-1$$

$$T_{oc,100} = 80 \quad K; \text{ cold end of cable}$$

APPENDIX A

Inner Conductor-Geometry

$$A_{ic,plating} = \pi \cdot (OR_{ic}^2 - (OR_{ic} - ic_{plated} \cdot t_{ic,plating})^2) \quad m^2; \text{ cross-sectional area of plating}$$

$$A_{ic,cladding} = \pi \cdot ((OR_{ic} - ic_{plated} \cdot t_{ic,plating})^2 - (OR_{ic} - ic_{plated} \cdot t_{ic,plating} - ic_{clad} \cdot t_{ic,cladding})^2) \quad m^2; \text{ cross-sectional area of cladding}$$

$$A_{ic,core} = \pi \cdot (OR_{ic} - ic_{plated} \cdot t_{ic,plating} - ic_{clad} \cdot t_{ic,cladding})^2 \quad m^2; \text{ cross-sectional area of core}$$

Inner Conductor-Energy Balance

$$T_{ic,1} = 300 \quad K; \text{ room-temperature end of cable}$$

$$q_{in,ic,plating,i} + q_{in,ic,cladding,i} + q_{in,ic,core,i} + q_{gen,ic,i} + q_{D,ic,i} = q_{out,ic,plating,i} + q_{out,ic,cladding,i} + q_{out,ic,core,i} \quad \text{for } i = 2 \text{ to } n-1$$

$$q_{in,ic,plating,i} = ic_{plated} \cdot \left[\frac{k_{ic,plating,i-1} + k_{ic,plating,i}}{2} \right] \cdot A_{ic,plating} \cdot \left[\frac{T_{ic,i-1} - T_{ic,i}}{dL} \right] \quad \text{for } i = 2 \text{ to } n-1$$

$$q_{in,ic,cladding,i} = ic_{clad} \cdot \left[\frac{k_{ic,cladding,i-1} + k_{ic,cladding,i}}{2} \right] \cdot A_{ic,cladding} \cdot \left[\frac{T_{ic,i-1} - T_{ic,i}}{dL} \right] \quad \text{for } i = 2 \text{ to } n-1$$

$$q_{in,ic,core,i} = \left[\frac{k_{ic,core,i-1} + k_{ic,core,i}}{2} \right] \cdot A_{ic,core} \cdot \left[\frac{T_{ic,i-1} - T_{ic,i}}{dL} \right] \quad \text{for } i = 2 \text{ to } n-1$$

$$q_{out,ic,plating,i} = ic_{plated} \cdot \left[\frac{k_{ic,plating,i} + k_{ic,plating,i+1}}{2} \right] \cdot A_{ic,plating} \cdot \left[\frac{T_{ic,i} - T_{ic,i+1}}{dL} \right] \quad \text{for } i = 2 \text{ to } n-1$$

$$q_{out,ic,cladding,i} = ic_{clad} \cdot \left[\frac{k_{ic,cladding,i} + k_{ic,cladding,i+1}}{2} \right] \cdot A_{ic,cladding} \cdot \left[\frac{T_{ic,i} - T_{ic,i+1}}{dL} \right] \quad \text{for } i = 2 \text{ to } n-1$$

$$q_{out,ic,core,i} = \left[\frac{k_{ic,core,i} + k_{ic,core,i+1}}{2} \right] \cdot A_{ic,core} \cdot \left[\frac{T_{ic,i} - T_{ic,i+1}}{dL} \right] \quad \text{for } i = 2 \text{ to } n-1$$

$$T_{ic,100} = 80 \quad K; \text{ cold end of cable}$$

RF MODEL

Constants

$$f = 3.9 \times 10^9 \quad \text{Hz; frequency of RF power}$$

$$\mu_0 = 4 \cdot \pi \cdot 1.0 \times 10^{-7} \quad \text{H/m; permeability of free space}$$

$$Z_0 = 50 \quad \text{ohms; impedance}$$

$$P_{cav} = 4.65 \quad \text{W; required power delivered to cavity}$$

$$\Gamma_{cav} = 0.94 \quad \text{reflection coefficient}$$

RF Attenuation Coefficients

$$\alpha_{ic,i} = \frac{\sqrt{f \cdot \mu_0 \cdot \rho_{c,i}}}{4 \cdot \sqrt{\pi} \cdot Z_0 \cdot OR_{ic}} \quad \text{for } i = 1 \text{ to } n \quad \text{inner conductor attenuation coefficients}$$

$$\alpha_{oc,i} = \frac{\sqrt{f \cdot \mu_0 \cdot \rho_{oc,i}}}{4 \cdot \sqrt{\pi} \cdot Z_0 \cdot IR_{oc}} \quad \text{for } i = 1 \text{ to } n \quad \text{outer conductor attenuation coefficients}$$

$$\alpha_{cable,i} = \alpha_{ic,i} + \alpha_{oc,i} + \alpha_D \quad \text{for } i = 1 \text{ to } n$$

APPENDIX A

RF Forward and Reflected Powers

$$P_{L,FWD,i} = P_{L,FWD,i+1} \cdot \exp(2 \cdot \alpha_{cable,i+1} \cdot dL) \quad \text{for } i=1 \text{ to } n-2 \quad W; \text{ forward power}$$

$$P_{L,REF,i} = P_{L,REF,i+1} \cdot \exp(-2 \cdot \alpha_{cable,i+1} \cdot dL) \quad \text{for } i=1 \text{ to } n-2 \quad W; \text{ reflected power}$$

$$P_{L,FWD,99} = P_{L,FWD,100} \cdot \exp\left[2 \cdot \alpha_{cable,100} \cdot \frac{dL}{2}\right] \quad W; \text{ forward power}$$

$$P_{L,REF,99} = P_{L,REF,100} \cdot \exp\left[-2 \cdot \alpha_{cable,100} \cdot \frac{dL}{2}\right] \quad W; \text{ reflected power}$$

$$P_{L,FWD,100} = \frac{P_{cav}}{1 - \Gamma_{cav}^2} \quad W; \text{ forward power}$$

$$P_{L,REF,100} = P_{L,FWD,100} \cdot \Gamma_{cav}^2 \quad W; \text{ reflected power}$$

RF Losses

$$P_{cable,1} = P_{L,FWD,1} \cdot \left[\exp\left(2 \cdot \alpha_{cable,1} \cdot \frac{dL}{2}\right) - 1 \right] + P_{L,REF,1} \cdot \left[1 - \exp\left(-2 \cdot \alpha_{cable,1} \cdot \frac{dL}{2}\right) \right] \quad W; \text{ cable power loss}$$

$$P_{cable,i} = P_{L,FWD,i} \cdot (\exp(2 \cdot \alpha_{cable,i} \cdot dL) - 1) + P_{L,REF,i} \cdot (1 - \exp(-2 \cdot \alpha_{cable,i} \cdot dL)) \quad \text{for } i=2 \text{ to } n-1 \quad W; \text{ cable power loss}$$

$$P_{cable,100} = P_{L,FWD,100} \cdot \left[\exp\left(2 \cdot \alpha_{cable,100} \cdot \frac{dL}{2}\right) - 1 \right] + P_{L,REF,100} \cdot \left[1 - \exp\left(-2 \cdot \alpha_{cable,100} \cdot \frac{dL}{2}\right) \right] \quad W; \text{ cable power loss}$$

$$P_{ic,i} = \frac{\alpha_{ic,i}}{\alpha_{cable,i}} \cdot P_{cable,i} \quad \text{for } i=1 \text{ to } n \quad W; \text{ inner conductor power loss}$$

$$P_{oc,i} = \frac{\alpha_{oc,i}}{\alpha_{cable,i}} \cdot P_{cable,i} \quad \text{for } i=1 \text{ to } n \quad W; \text{ outer conductor power loss}$$

$$P_{D,i} = \frac{\alpha_D}{\alpha_{cable,i}} \cdot P_{cable,i} \quad \text{for } i=1 \text{ to } n \quad W; \text{ dielectric power loss}$$

$$q_{gen,ic,i} = P_{ic,i} \quad \text{for } i=1 \text{ to } n \quad W$$

$$q_{gen,oc,i} = P_{oc,i} \quad \text{for } i=1 \text{ to } n \quad W$$

Dielectric Temperature Distribution

$$A_D = \pi \cdot (OR_D^2 - IR_D^2) \quad m^2; \text{ cross-sectional area of dielectric}$$

$$V_{D,1} = A_D \cdot \frac{dL}{2} \quad m^3; \text{ nodal volume of dielectric}$$

$$V_{D,i} = A_D \cdot dL \quad \text{for } i=2 \text{ to } n-1 \quad m^3; \text{ nodal volume of dielectric}$$

$$V_{D,100} = A_D \cdot \frac{dL}{2} \quad m^3; \text{ nodal volume of dielectric}$$

$$\dot{q}_{D,i} = \frac{P_{D,i}}{V_{D,i}} \quad \text{for } i=1 \text{ to } n \quad W/m^3; \text{ volumetric generation rate}$$

$$T_{ic,i} = \frac{-\dot{q}_{D,i}}{4 \cdot k_{D,i}} \cdot IR_D^2 + C1_i \cdot \ln(IR_D) + C2_i \quad \text{for } i=1 \text{ to } n$$

$$T_{oc,i} = \frac{-\dot{q}_{D,i}}{4 \cdot k_{D,i}} \cdot OR_D^2 + C1_i \cdot \ln(OR_D) + C2_i \quad \text{for } i=1 \text{ to } n$$

APPENDIX A

$$q_{D,ic,1} = k_{D,1} \cdot 2 \cdot \pi \cdot IR_D \cdot \frac{dL}{2} \cdot \left[\frac{-\dot{q}_{D,1} \cdot IR_D}{2 \cdot k_{D,1}} + \frac{C1_1}{IR_D} \right] \quad W$$

$$q_{D,oc,1} = -k_{D,1} \cdot 2 \cdot \pi \cdot OR_D \cdot \frac{dL}{2} \cdot \left[\frac{-\dot{q}_{D,1} \cdot OR_D}{2 \cdot k_{D,1}} + \frac{C1_1}{OR_D} \right] \quad W$$

$$q_{D,ic,i} = k_{D,i} \cdot 2 \cdot \pi \cdot IR_D \cdot dL \cdot \left[\frac{-\dot{q}_{D,i} \cdot IR_D}{2 \cdot k_{D,i}} + \frac{C1_i}{IR_D} \right] \quad \text{for } i=2 \text{ to } n-1 \quad W$$

$$q_{D,oc,i} = -k_{D,i} \cdot 2 \cdot \pi \cdot OR_D \cdot dL \cdot \left[\frac{-\dot{q}_{D,i} \cdot OR_D}{2 \cdot k_{D,i}} + \frac{C1_i}{OR_D} \right] \quad \text{for } i=2 \text{ to } n-1 \quad W$$

$$q_{D,ic,100} = k_{D,100} \cdot 2 \cdot \pi \cdot IR_D \cdot \frac{dL}{2} \cdot \left[\frac{-\dot{q}_{D,100} \cdot IR_D}{2 \cdot k_{D,100}} + \frac{C1_{100}}{IR_D} \right] \quad W$$

$$q_{D,oc,100} = -k_{D,100} \cdot 2 \cdot \pi \cdot OR_D \cdot \frac{dL}{2} \cdot \left[\frac{-\dot{q}_{D,100} \cdot OR_D}{2 \cdot k_{D,100}} + \frac{C1_{100}}{OR_D} \right] \quad W$$

Overall Performance Metrics

$$\dot{q}_{loss,total} = \frac{\sum_{i=1}^n (P_{cable,i})}{L} \quad W/m; \text{ cable loss rate}$$

$$\dot{q}_{loss,ic} = \frac{\sum_{i=1}^n (P_{ic,i})}{L} \quad W/m; \text{ inner conductor loss rate}$$

$$\dot{q}_{loss,D} = \frac{\sum_{i=1}^n (P_{D,i})}{L} \quad W/m; \text{ dielectric loss rate}$$

$$\dot{q}_{loss,oc} = \frac{\sum_{i=1}^n (P_{oc,i})}{L} \quad W/m; \text{ outer conductor loss rate}$$

$$q_{80K} = q_{out,oc,plating,99} + q_{out,oc,core,99} + q_{out,ic,plating,99} + q_{out,ic,cladding,99} + q_{out,ic,core,99} + P_{ic,100} + P_{D,100} + P_{oc,100}$$

W; heat load to 80 K

APPENDIX B

Table I lists the cables that were analyzed using the analysis model. They are listed in increasing outer diameter size represented in thousandths of an inch by the last three numbers in the part number. Included in the list is each cable's inner and outer conductor materials and dielectric material. These cables are from Precision Tube and Micro-Coax. Times Microwave offers braided cables of similar size and materials, thus its braided cables are represented within this list. Coaxial cable that is available from Andrew Corp is also represented by such cables as the BP50250 and the UFB311A.

Cable	I.C. Material	Dielectric Material	O.C. Material
PT MiniLossPlus RH50141	SPC	LDPTFE	1100 AL
PT SoftFormPlus AH50141	SPCW	Solid PTFE	1100 AL
PT SoftFormPlus BH50141	SPC	Solid PTFE	1100 AL
PT SoftForm AP50141	SPCW	Solid PTFE	99.9% Cu
PT SoftFormPlus BP50141	SPC	Solid PTFE	99.9% Cu
MC AlumiLine UT-141A-AL-TP-L	SPC	LDPTFE	Tin/AL
MC AlumiLine UT-141A-AL-TP	SPCW	Solid PTFE	Tin/1100 AL
MC UTiForm UT-141-Form	SPCW	Solid PTFE	Tin SPC
MC UTiForm UT-141C-Form	SPC	Solid PTFE	Tin SPC
MC UTiForm UT-141C-Form-LL	SPC	LDPTFE	Tin SPC
MC UTiFlex UFB142A	SPC	UltraLDPTFE	SPC
MC UTiFlex UFA147A	SPC	LDPTFE	SPC
MC UTiForm UT-250C-Form-LL	SPC	LDPTFE	Tin SPC
PT SoftFormPlus RH50250	SPC	LDPTFE	1100 AL
PT SoftFormPlus BH50250	SPC	Solid PTFE	1100 AL
PT SoftForm BP50250	SPC	Solid PTFE	99.9% Cu
MC AlumiLine UT-250A-AL-TP	SPC	Solid PTFE	Tin/1100 AL
MC UTiFlex UFB311A	SPC	UltraLDPTFE	SPC
PT SoftFormPlus NH50325	SPC	Solid PTFE	1100 AL

Table 1: Simulated Coaxial Cable Types (high-lighted cables are the hand-formable type, others are the braided shield design)

SPC: Silver-Plated Copper
 SPCW: Silver-Plated Copper-Clad Steel
 AL: Aluminum Cu: Copper
 PTFE: Solid Polytetrafluoroethylene
 LDPTFE: low-density PTFE
 UltraLDPTFE: Ultra low-density PTFE
 PT: Precision Tube
 MC: Micro-Coax

APPENDIX B

Each cable from Table 1 was simulated within the analysis model. For each cable, the cable length which resulted in a minimum continuous-wave (CW) heat load on the 80K intercept was found. For each cable, Fig.2 shows the optimum length while Fig.3 shows the heat load at this optimum length.

There are two practical cable lengths to choose from for the cable routing. One of these, 0.35m, results from a cable arrangement as shown in Fig.1. The other length, 0.25m, is the length resulting from routing the cable straight out of the cryostat, parallel to the bellows section. Thus, Fig.4 and Fig.5 show the results from simulations at 0.25m and 0.35m respectively.

Figure 2

Optimum Cable Length for CW Operation

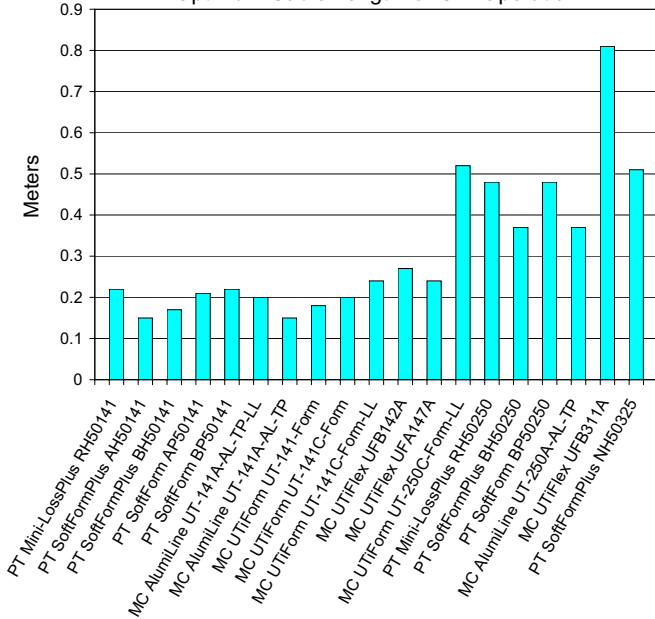


Figure 3

Heat Loss Rates for Optimum Cable Length

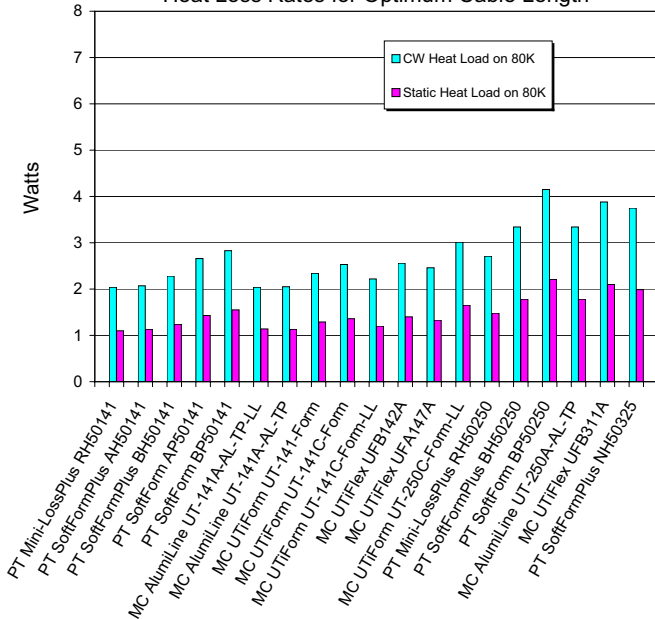


Figure 4

Heat Loss Rates for 0.25m Cable

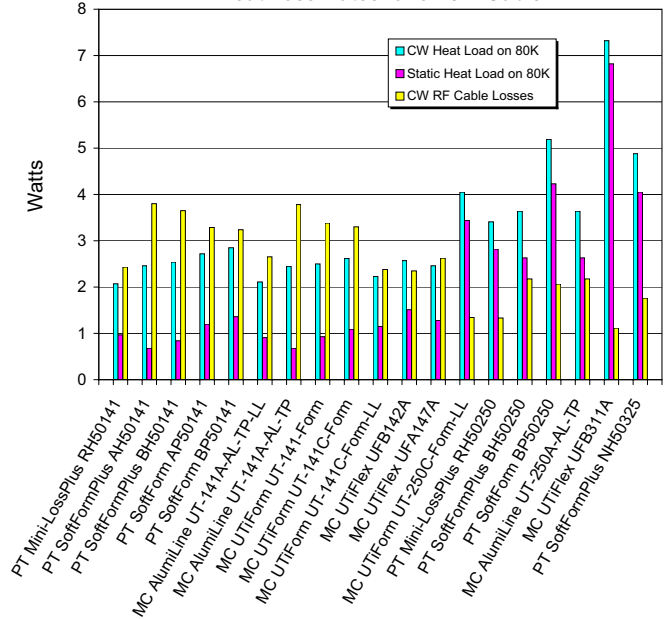
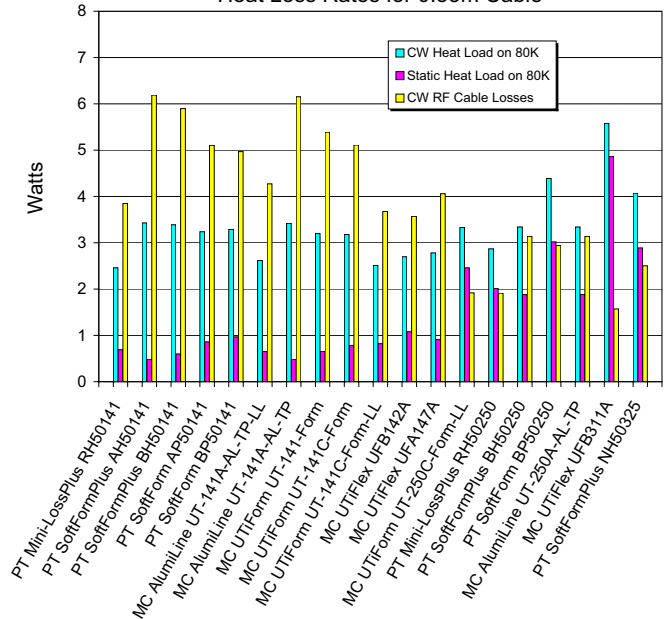


Figure 5

Heat Loss Rates for 0.35m Cable



APPENDIX C
SiO₂ Coaxial Cable
Heat Load Simulation Results

